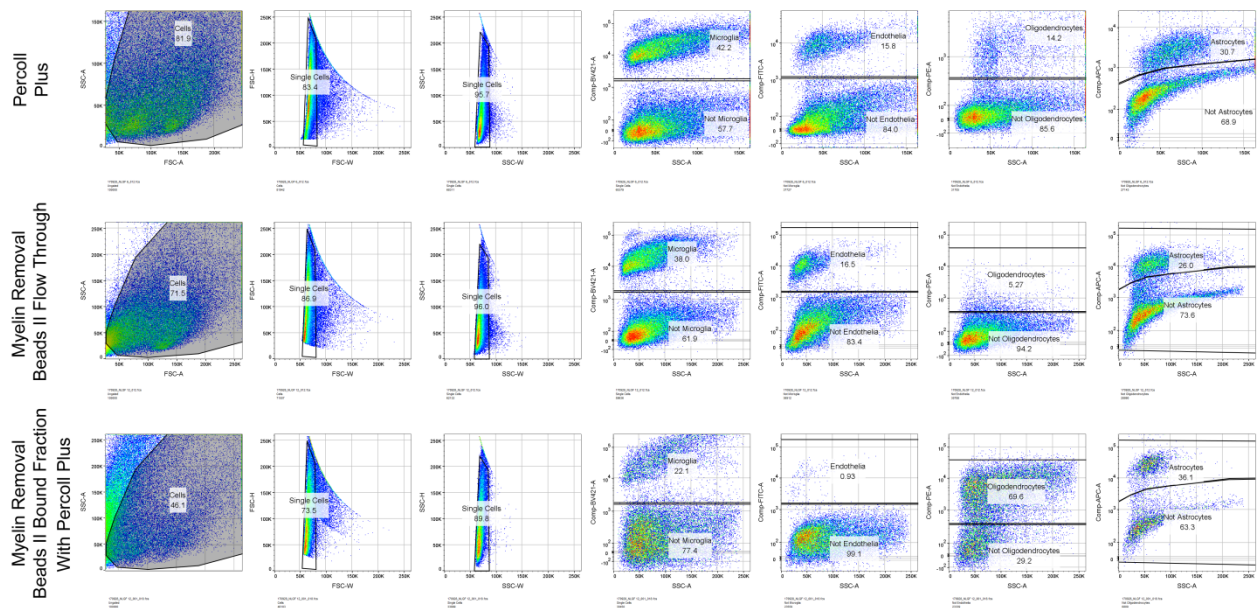
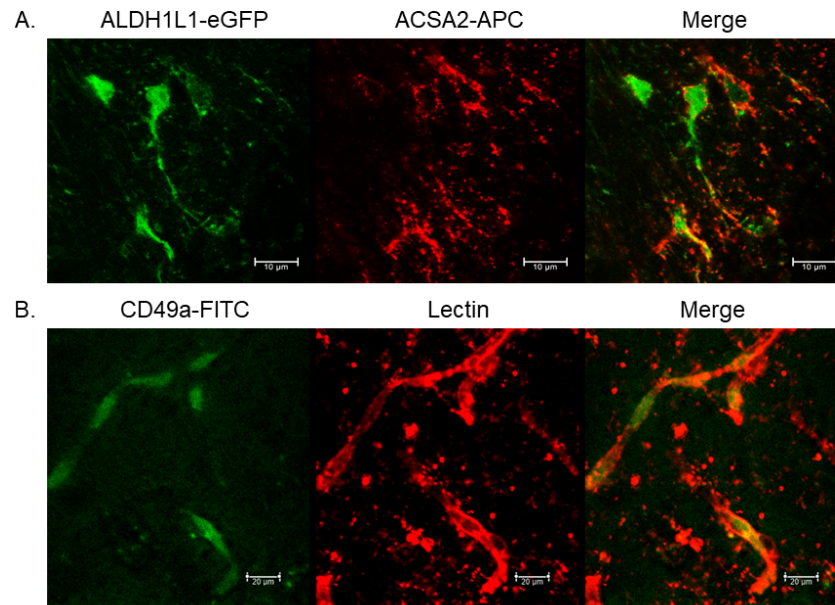


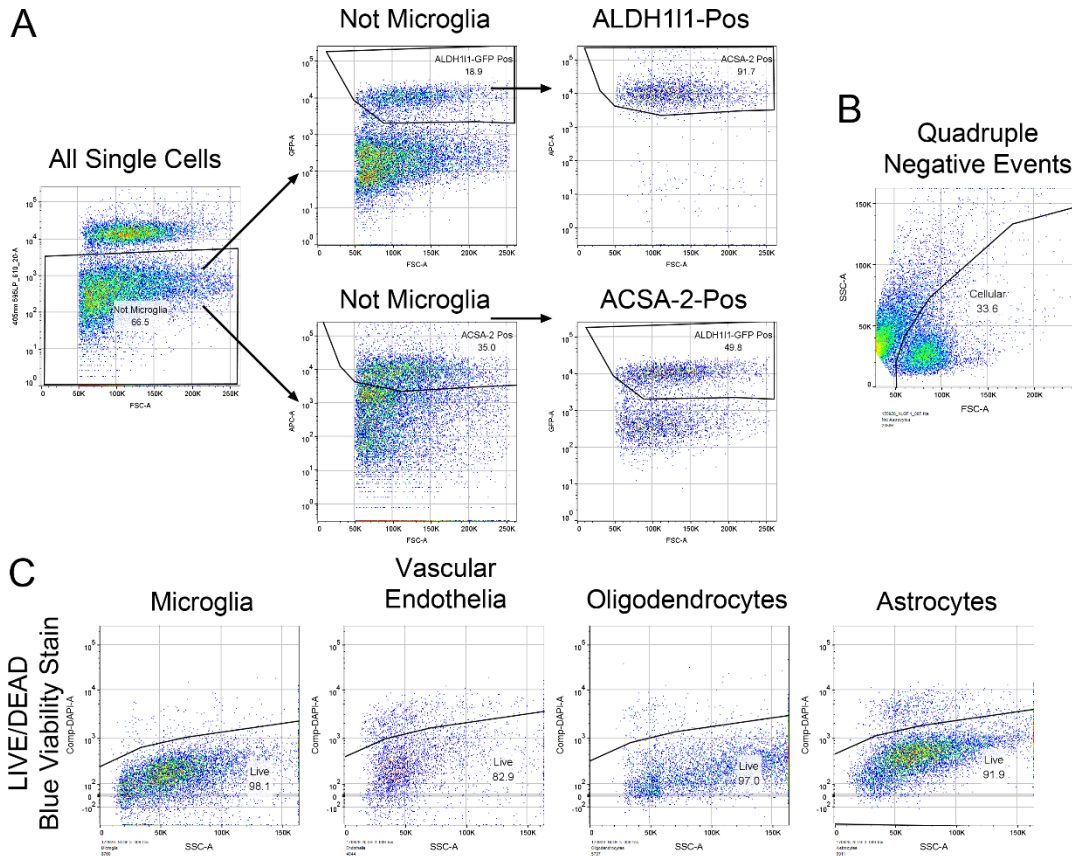
Supplemental Figures



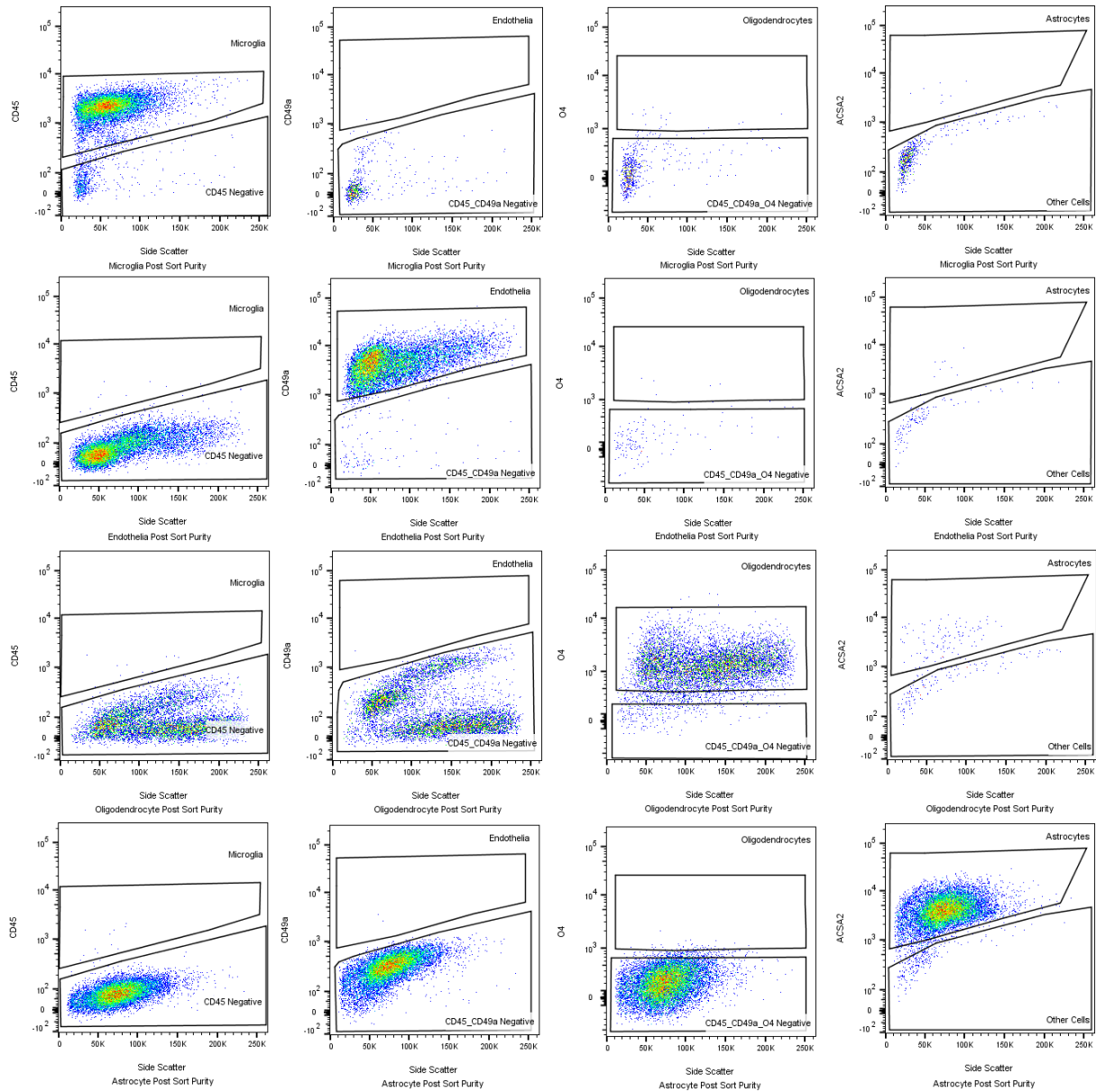
Supplemental Figure 1: Representative FACS data showing Concurrent Brain cell type Acquisition using either Percoll PLUS (top row) or myelin removal beads (bottom two rows). Debris clean up using Percoll PLUS yield microglia (CD45+), vascular endothelia (CD49a+), oligodendrocytes (O4+) and astrocytes (ACSA-2+). Debris removal with myelin removal beads II (Flow through, middle row) yields all cell types except oligodendrocytes. FACS analysis of the bound fraction from myelin removal beads II shows that some microglia, astrocytes, and all oligodendrocytes are initially bound to the column showing how if oligodendrocytes are required the bound fraction must first be eluted and debris removed using Percoll PLUS.



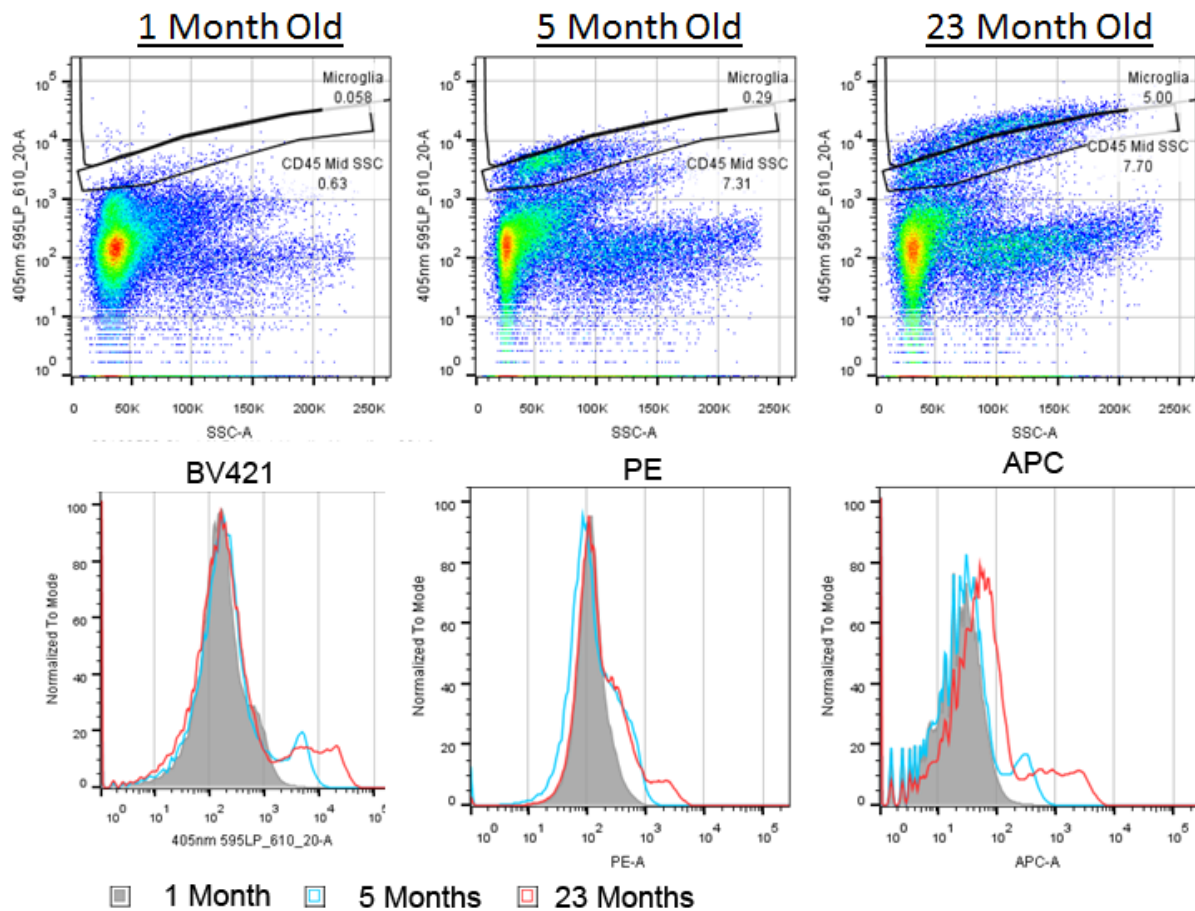
Supplemental Figure 2: Representative images of brain sections stained with flow cytometry conjugated fluorescent antibodies with their cell-type markers. (A) Fluorescent image of ACSA-2 staining the cellular membrane of ALDH1L1-GFP positive astrocytes. **(B)** Fluorescent image of CD49a staining endothelial cells as marked by Lectin. Scale bar in A: 10 μm ; in B: 20 μm .



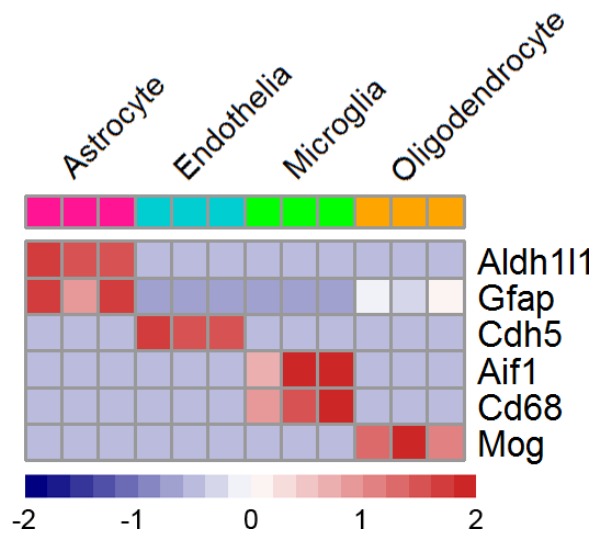
Supplemental Figure 3: Comparison of astrocytes isolated using the ALDH111-eGFP reporter and the anti-ACSA-2 antibody. (A) The ALDH111-eGFP reporter line was used to ascertain whether the anti-ACSA-2 antibody labeled astrocytes. All non-microglial cells were gated for GFP or ACSA-2 positivity. Nearly all ALDH111-eGFP cells were also ACSA-2 positive while only about 50% of ACSA-2 positive cells were ALDH111-eGFP positive suggesting that ACSA-2 labels more astrocytes than ALDH111-eGFP at 5 months of age. N=2. **(B)** Representative flow cytometry plot of quadruple negative events by forward- and side-scatter suggesting about one-third of quadruple negative events are cellular and may represent additional cell types. A portion of these events may however be blood which remains from incomplete perfusions. **(C)** Representative flow cytometry plot of cell viability using the LIVE/DEAD Blue viability dye when looking at each cell population. Data summarized in Table 1.



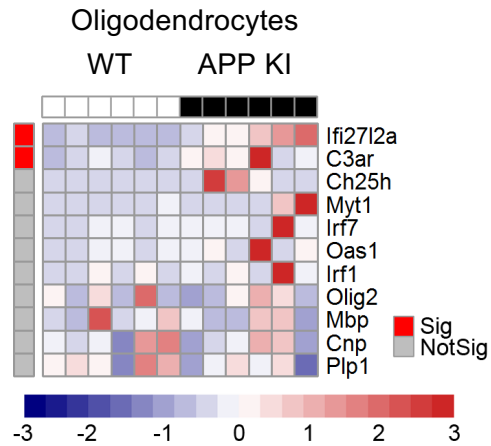
Supplemental Figure 4: Representative plots of post sort purity gating strategy used to quantify percentage of sorted cell contaminants. Following CoBrA sorting, of six month old C57BL/6J mice, each cell fraction was rerun on the Aria II to determine sort purity. Gates were drawn around single cells and sort gates were applied to analyze each cell population's contaminants. Notably there is a rare occurrence of either microglia, endothelia, oligodendrocytes, or astrocytes contaminating one another. However, each group contains a small percentage of quadruple negative cells or cellular debris contaminants. Flow plots represent one experiment where N=3. Data summarized in Table 1.



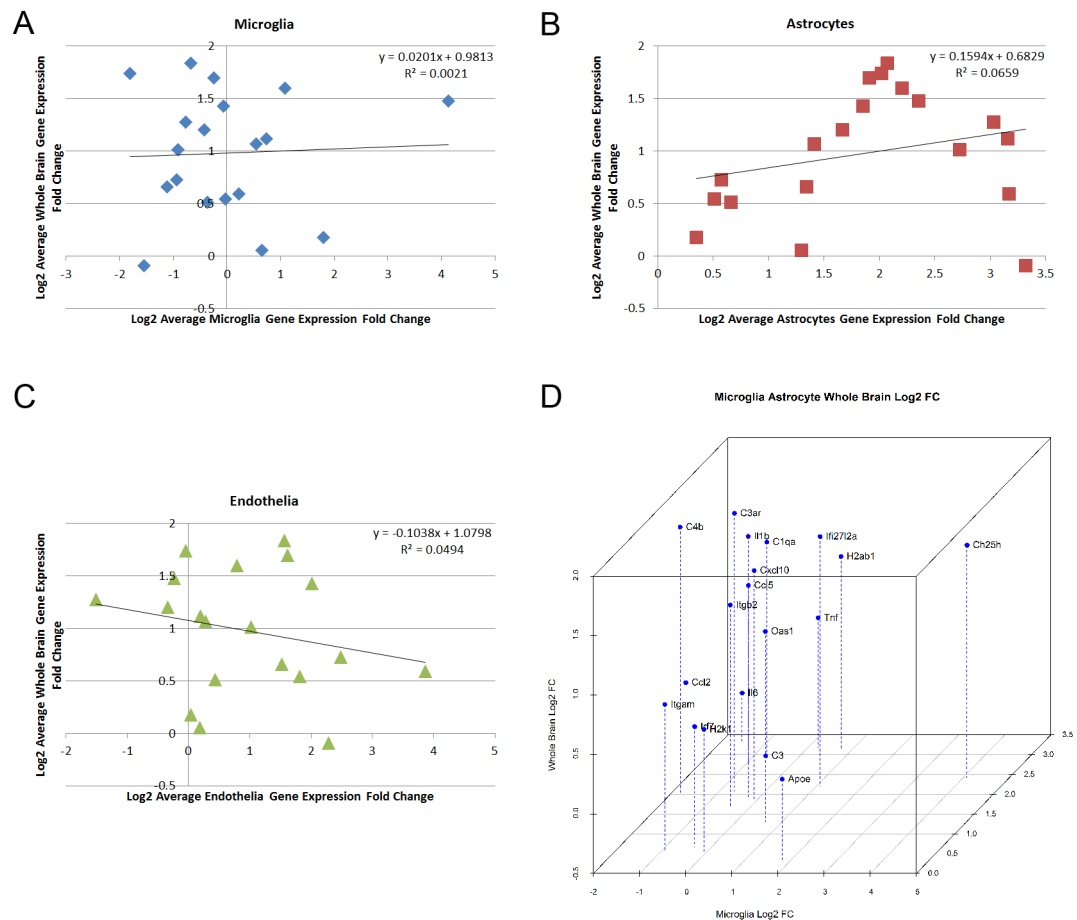
Supplemental Figure 5: Representative flow cytometry plots showing increases of autofluorescence with age. At one month (grey) almost no cells are autofluorescent in the BV605 (top panels), BV421, PE, or APC (bottom panels) channels. At five months (blue line) autofluorescence is easily observable, and at 23 months (red line) a large proportion of cells are autofluorescent in all channels.



Supplemental Figure 6: Heatmap comprised of relative expression qRT-PCR data from FACS sorted astrocytes (*Aldh1l1*, *Gfap*), vascular endothelia (*Cdh5*), microglia (*Aif1*, *Cd68*), and oligodendrocytes (*Mog*). N=3.



Supplemental Figure 7: Heatmap of qRT-PCR data from Concurrent Brain cell type Acquisition isolated oligodendrocytes. Oligodendrocyte-specific genes analyzed for O4-positive cells. Sig. = $P < 0.05$ (Red) and Not Sig. = $P \geq 0.05$ (Grey), t-Test. N=6/genotype.



Supplemental Figure 8: Correlation analysis of qRT-PCR fold change data from Figure 4A correlating each cell type with bulk brain data. (A) Microglia versus bulk brain yields a flat correlation suggesting that microglia are not the primary cause of transcriptional changes of observed genes in the bulk brain. **(B)** Astrocytes versus bulk brain yields a positive correlation suggesting that astrocytes are a major driver of transcriptional changes of observed genes in the bulk brain. **(C)** Endothelia versus bulk brain yields a negative correlation suggesting that endothelia are not the primary cause of transcriptional changes of observed genes in the bulk brain. **(D)** A 3-dimensional scatter-plot of microglia (X-axis), bulk brain (Y-axis), and astrocytes (Z-axis) showing that genes expressed highest in bulk brain are also expressed highly in astrocytes and not necessarily microglia.